



THE UNIVERSITY *of* EDINBURGH
**School of Physics
and Astronomy**

**2025 Summer Project
Probing Sensitivities of Sterile Neutrino
Oscillation Parameters at DUNE using
GLoBES**

Paolo Minhas
June - July 2025

Abstract

The project shows the improvement in sensitivity to neutrino oscillation parameters such as δ_{CP} compared to previous neutrino oscillation experiments. This is further explored in relation to sterile neutrino oscillation parameters Δm_{14}^2 and $\sin^2 \theta_{24}$, and the large increase in sensitivity due to the near detector especially. This involved simulating the detector response at the far and near detectors and then combining for overall sensitivities. This was then compared to the same calculation as performed in the DUNE technical design report [1].

Declaration

I declare that this project and report is my own work.

Signature:

Supervisor: Dr. G. Vitti Stenico

Date: 24/06/2025
Summer Project

Lay Summary

This summer project estimates the sensitivity of the Deep Underground Neutrino Experiment (DUNE) to neutrino oscillations, in particular sterile neutrino parameters. A sterile neutrino is a theoretical fourth additional neutrino that cannot be detected like a standard model neutrino as it would not interact via the weak force. If it were to exist, using neutrino oscillation and detector simulations we predict what the data would look like, and then whether we could distinguish the difference between this and the standard model. It was found that the near detector is especially sensitive to certain sterile neutrino parameters due to a oscillation wavelength similar to the distance of the detector from the source, so a maximum would occur at the detector. Despite recent discoveries that suggest a sterile neutrino is not the most likely solution to discrepancies seen at previous neutrino oscillation experiments (most famously LSND [2]), it is still worth constraining what its potential effects would be on results at DUNE when it comes online in 2027.

Personal Statement

In this project I learned new skills as well as applying knowledge learned in my degree - especially from the last year (year 4). It was particularly exciting to get to learn how to use C and GLoBES - I had had a chance to use some C when using ROOT in a previous project, but this project allowed me to learn more about compilers, makefiles and memory assignment (via segmentation faults). I learned how to use visual studio code more effectively and got more experience with the command-line and vim. I also was given the opportunity to look through the theory behind neutrino oscillations in much more detail, looking at the notes written by E. Lisi over the course of the project. Finally I learned more about statistical methods - particularly how a chi squared test is implemented practically in particle physics - all of which I found invaluable knowledge to gain.

Acknowledgements

I would like to thank Dr Gabriela Vitti Stenico, my supervisor, for her help and guidance with this project, and for providing me with the resources to do this project. I would also like to thank Dr Miquel Nebot-Guinot, Dr Cheryl Patrick and Dr Pedro Pasquini for their further assistance on the DUNE project and the physics behind it, as well as supervising a previous project on DUNE that greatly helped me with this one. Thank you to the School of Physics and Astronomy at the University of Edinburgh for the funding this project via the Career Development Summer Scholarships, and the DUNE collaboration.

Contents

1	Introduction	2
2	Background	3
3	Simulation and Analysis Techniques	6
4	Results & Analysis	7
4.1	The Standard Model	7
4.2	Validating the Sterile Neutrino Engine	8
4.3	Implementing the near detector	9
5	Conclusions	10
A	Code	14
B	The Sterile Neutrino Implementation in GLoBES	14
C	The Algorithm	15
D	Further results	15

1 Introduction

The Deep Underground Neutrino Experiment (DUNE) is a long baseline neutrino oscillation experiment in the USA, that looks to detect neutrinos oscillating between flavours over a roughly 1300km baseline [1]. This paper seeks to find the theoretical sensitivity of the DUNE detectors (near and far) to not only standard model neutrino oscillation parameters, but those additionally for a sterile neutrino. This is done by producing χ^2 plots of parameters and finding regions of acceptance at a 90% or 99% confidence level.

Simulations of the beam production and then true data in the near and far detectors are made. The relative proportions of each neutrino flavour are compared between the near detector (acting as essentially a detector before neutrinos oscillate with the exception of some sterile neutrino parameters discussed later) and the far detector. Therefore, when proportions change it suggests one flavour of neutrino has oscillated to another - we can look at appearance or disappearance of neutrinos of each flavour to build the overall picture. Due to the underlying matrix equation representing the oscillation, certain channels (e.g. electron neutrino appearance) are more crucial than others to determine certain parameters.

Due to the difficulty of creating a pure single-flavour neutrino beam, there are many uncertainties in the beam content at the near detector. The beam is made up of mostly electron neutrinos (with some muon neutrinos and few tau neutrinos), and when in forward horn (arranged for neutrinos rather than antineutrinos) is mostly neutrinos, not antineutrinos - nonetheless this is still a mix of all six possibilities [3]. The figure below shows the beam production and near detector facility at Fermilab near Chicago. This schematic is important in this report as it shows that the neutrino source is not a singular point, but a range across the decay pipe. This effect is negligible 1300km away at the far detector but important when simulating the near detector.

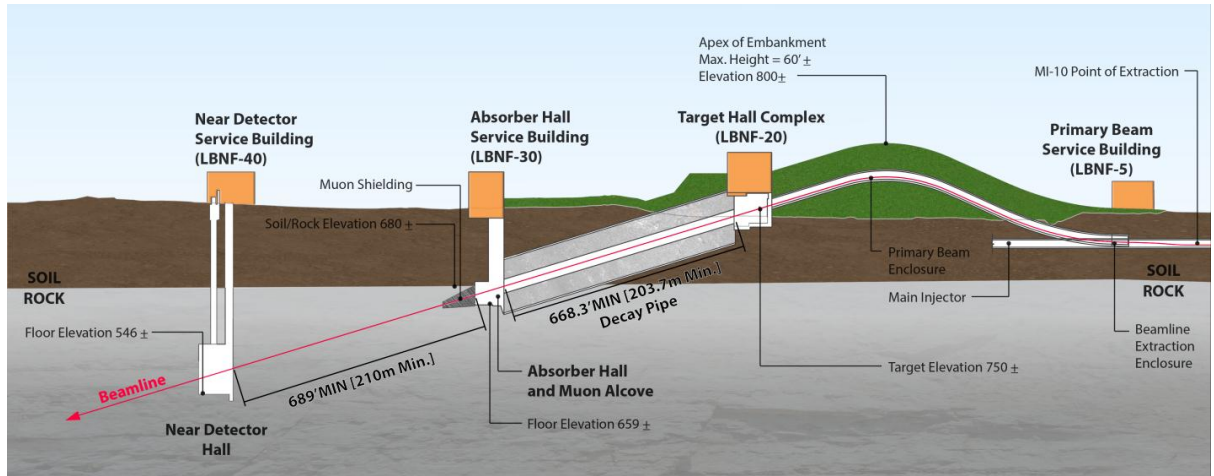


Figure 1: A schematic of the DUNE beamline taken from [3]. The decay pipe is visible and covers nearly 700m before another 700m to the near detector itself. Neutrino production happens across the entire length of the decay pipe.

2 Background

Neutrino oscillations were first postulated by Pontecorvo in 1957 [4], which he finalised 10 years later [5] and then was confirmed to occur in subsequent years independently [6]. Before this it was assumed that neutrinos were massless [7], but when given a small mass, flavour transitions can occur via oscillation. They occur as a result of the coexistence of flavour and mass eigenstates - each flavour (electron, muon tau for the 3 generations in the standard model) is made up of a superposition of mass states. These mass eigenstates travel at different speeds due to the different masses of the states, and therefore the ratio of each mass state changes, therefore changing the flavour of the neutrino. This means the observed flavour appears to oscillate as the neutrino travels, as the mass eigenstates propagate through space (whereas we only observe the flavour eigenstates).

This can be explored in a two neutrino model, before expanding to three, and later four.

$$\begin{pmatrix} |\nu_e\rangle \\ |\nu_\mu\rangle \end{pmatrix} = \begin{pmatrix} \cos\theta & \sin\theta \\ -\sin\theta & \cos\theta \end{pmatrix} \begin{pmatrix} |\nu_1\rangle \\ |\nu_2\rangle \end{pmatrix}$$

Hence the flavour eigenstates can be represented as a superposition of the mass eigenstates.

$$|\nu_e\rangle = \cos\theta|\nu_1\rangle + \sin\theta|\nu_2\rangle$$

$$|\nu_\mu\rangle = -\sin\theta|\nu_1\rangle + \cos\theta|\nu_2\rangle$$

The oscillation probability from one flavour to another (in natural units) is therefore:

$$P_{\nu_\alpha \rightarrow \nu_\beta} = \sin^2(2\theta) \sin^2\left(\frac{\Delta m^2 L}{4E}\right)$$

where

L = DUNE baseline (c. 1300km) (length between the near and far detectors)

E = The beam energy describes the energy of interactions

$$\Delta m_{ij}^2 = \text{mass splitting term} - \Delta m_{ij}^2 = \Delta m_i^2 - \Delta m_j^2$$

θ = oscillation phase angle describing the frequency of oscillations over space

A conversion factor of 1.267 must be applied inside the bracket when using ‘lab’ units (E in GeV, m in eV², and L in km). In matter more factors must be considered. This results in a similar equation, but with altered angle and mass terms.

$$P_{\nu_e \rightarrow \nu_\mu} = \sin^2(2\theta_m) \sin^2\left(\frac{\Delta m_m^2 L}{4E}\right)$$

Where $\sin^2(2\theta_m) = \frac{\sin^2(2\theta)}{\left(\cos(2\theta) - \frac{2EV}{\Delta m^2}\right)^2 + \sin^2(2\theta)}$, $\Delta m_m^2 = \Delta m^2 \sqrt{\left(\cos(2\theta) - \frac{2EV}{\Delta m^2}\right)^2 + \sin^2(2\theta)}$
and $V = \sqrt{2}G_F N_e$.

Two new matter terms have been introduced - G_F & N_e . G_F is the Fermi coupling constant - a constant of nature that defines the strength of the weak force. N_e is the electron number density of the medium - the matter effect primarily affects electron neutrinos, therefore modifying all oscillation probabilities as this is not a symmetrical effect. In a 3 neutrino, and eventually a 3+1 neutrino model, the oscillation probability becomes more complex with more terms, but it follows the same motivation as the 2 flavour oscillation described above (just with 3×3 or 4×4 matrices).

The two most important oscillation probabilities at DUNE are muon neutrino disappearance ($\nu_\mu \rightarrow \nu_\mu$) and electron neutrino appearance ($\nu_\mu \rightarrow \nu_e$) (due to the beam content, and magnitudes of neutrino mixing). It is clear that the mass eigenstates have different masses [8] but we are still uncertain of the ordering of these states. Experiments have worked to constrain the mass splitting terms but as this represents Δm_{23}^2 we do not know the sign of the mass difference. This leaves two options for the ordering of mass eigenstates.

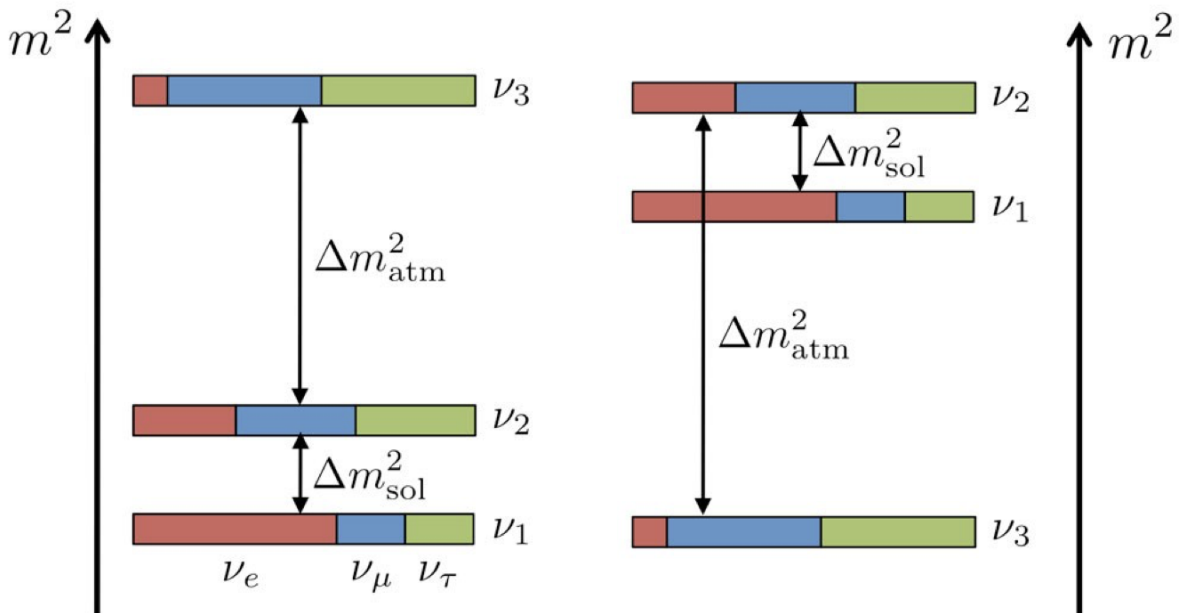


Figure 2: The two options for mass ordering - normal and inverted hierarchy on the left and right hand sides respectively. The colours refer to the superpositions of neutrino flavour eigenstates in each mass eigenstate - it can be seen that the first mass state is dominated by the electron neutrino, whereas the third by the muon and tau flavours. The mass of the flavour eigenstates can be proven by summing the total proportions of each mass eigenstate present in a flavour state. Taken from [9].

In inverted hierarchy, the third mass state is lighter than the first and second instead of the intuitive arrangement of the natural ordering. This would change the event spectra for different neutrino flavours detected at the far detector. The mass splitting terms describe the smaller solar mass splitting Δm_{sol}^2 or Δm_{12}^2 and the atmospheric mass splitting Δm_{atm}^2 or Δm_{23}^2 as can be seen in Figure 2.

The sterile neutrino is a theoretical fourth neutrino [10] - the sterile neutrino we refer to in this report does not interact via the weak force, is a part of a 3+1 neutrino model (ignoring any non-standard interactions) and is heavy relative to the standard model neutrinos. This means the sterile neutrino mass splitting terms have a higher order. This can be visualised in Figure 3, where the value for Δm_{14}^2 is around 1 eV^2 .

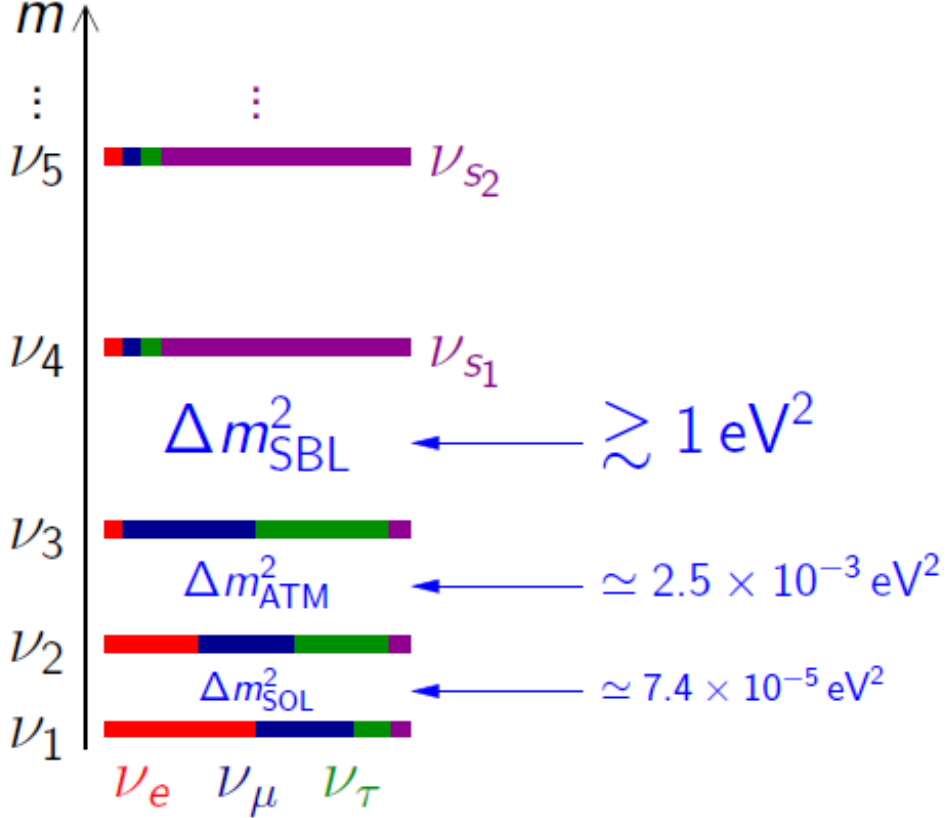


Figure 3: The sterile neutrino added to the mass ordering chart. $\Delta m_{\text{SBL}}^2 = \Delta m_{41}^2 = \Delta m_4^2 - \Delta m_1^2$ with SBL referring to the short baseline. Figure taken from [11].

This short baseline mass splitting term is named so due to the significance of its magnitude. When revisiting the oscillation probability formula from above, it becomes clear that when substituting in values for L and for E at the near detector, there will be an oscillation maximum that correlates with the sterile neutrino. Therefore it should be expected that sensitivity will be increased by the near detector [12]. The disappearance probability, using an effective two flavour approximation (as the masses of standard model neutrinos are much smaller) can be calculated (although the true calculations used in the code were much more complex):

$$P_{\nu_\mu \rightarrow \nu_\mu} \approx 1 - \sin^2(2\theta_{\mu\mu}) \sin^2 \left(\frac{\Delta m_{41}^2 L}{4E} \right)$$

and the appearance probability:

$$P_{\nu_\mu \rightarrow \nu_e} \approx \sin^2(2\theta_{\mu e}) \sin^2\left(\frac{\Delta m_{41}^2 L}{4E}\right)$$

with regard to muon neutrinos.

DUNE will also search for Charge-Parity (CP) violation - which in this context refers to an asymmetry in neutrino oscillations favouring neutrinos over antineutrinos as a ‘final state’ (at the far detector). The sensitivity to this is dependent on how accurately δ_{CP} can be measured (the CP violating phase [13], a quantitative measure of how asymmetric the oscillations are over all events).

3 Simulation and Analysis Techniques

Simulations were created using the General Long Baseline Experiment Simulator (GLoBES) [14], a software package of C libraries specifically made to simulate neutrino oscillation experiments. The output was interpreted using numpy in python, and plotted with matplotlib. Some graphs were also plotted in Mathematica using the same process. The final code can be found at [15]. The χ^2 test statistic is a statistical test that determines how closely test data align with a theoretical model (or any comparison between two data sets). It can be motivated by taking the concept of a least-squares fit (the model minus the data, all squared) then weighted based on the size of its uncertainty:

$$\chi^2 = \sum_{\text{all bins}} \frac{(x_{true} - x_{test})^2}{\sigma_{test}^2}$$

This value is calculated with respect to all the parameters left free in the simulation, and then the χ^2 is then minimised using a minimising algorithm. The value of the parameter at the minimised χ^2 function is taken. Then these values are to calculate the final χ^2 test with the parameters being investigated left free. By plotting this on a smear matrix, it is possible to visualise the regions in which the chi squared value is lower - meaning that there is less of a discrepancy between the true and test data and DUNE detectors would be more sensitive.

DUNE measurement power is measured using Bayesian statistics, by comparing the theoretical simulation of events (true) and then an alternative hypothesis (test). The χ^2 result can be easily converted into a significance level which can be interpreted easily. Several comparisons were made in this report. The null hypothesis of normal mass ordering was compared to an alternative hypothesis of inverted ordering, as well as a null hypothesis of a three neutrino model compared to a four neutrino model with a sterile neutrino.

In this project, initially the χ^2 statistic was calculated by a simple algorithm, but by implementing the GLoBES built-in *ChiMultiExp* function, a more robust and faster calculation was performed for all the data. Values of known parameters in the simulation were taken from the most recent data possible at NuFit [16]. For a detailed breakdown of the logic used in the code, please see the appendix. The sterile neutrino was simulated with the addition of the SNU library made by Joachim Kopp from the Max Planck Institute für Kernphysik [17] - which is detailed in the appendix as well.

4 Results & Analysis

4.1 The Standard Model

DUNE is able to provide much higher sensitivity than previous neutrino oscillation detectors such as T2K [18] due to its energy baseline. This results in a more confined acceptance area for oscillation parameters on the χ^2 graph. The graph in Figure 4 shows the sensitivity of these detectors when looking at a null hypothesis of normal ordering and an alternative hypothesis of inverted ordering. DUNE has a smaller acceptance region meaning there are less values that can prove normal ordering is not valid. This means inverted ordering van be more likely ruled out (or accepted) using DUNE.

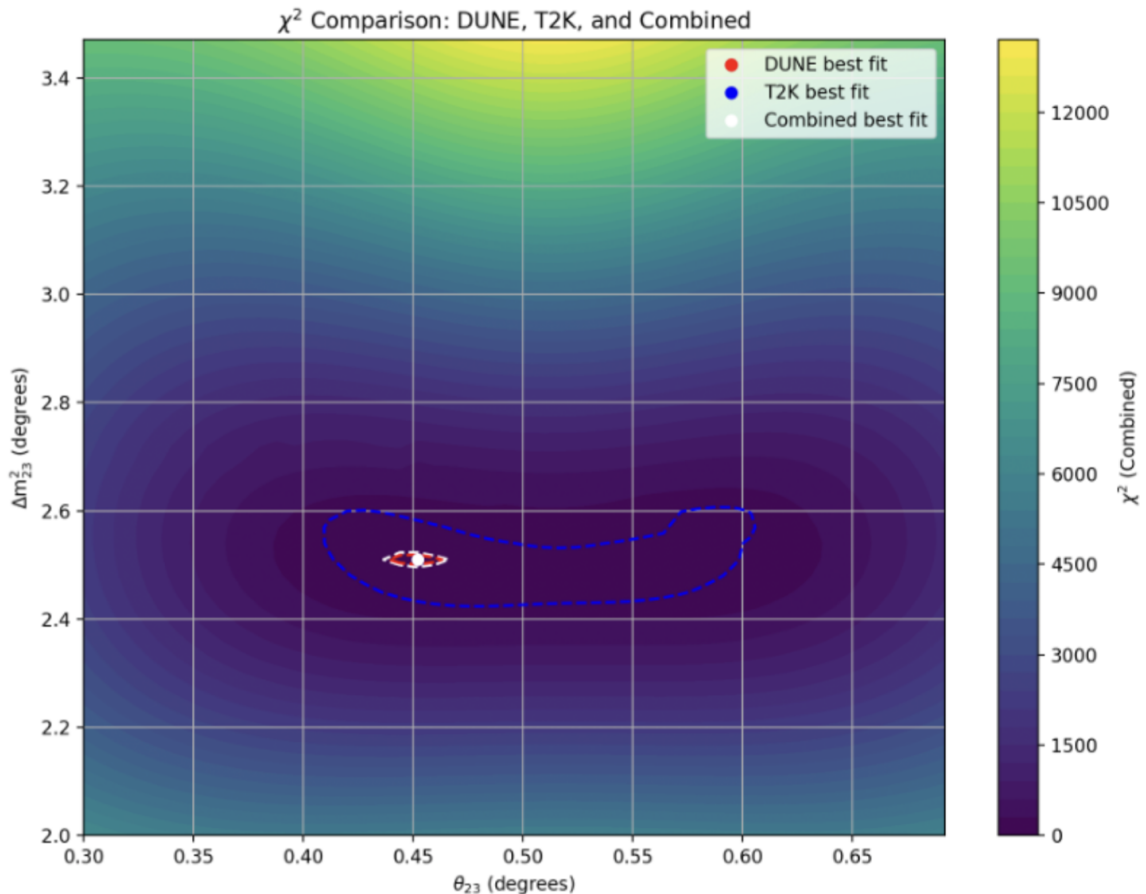


Figure 4: The acceptance ranges for 99% acceptance level. The colour gradient represents the combined χ^2 , which can be seen to be similar to that of only DUNE, especially compared to T2K. This means by combining DUNE’s data with a detector of lower sensitivity, the data still has a much greater overall sensitivity. In this case the sensitivity refers to that of the Δm_{23}^2 and $\sin \theta_{23}$ parameters, when taking a null hypothesis of normal mass hierarchy and an alternate hypothesis of inverted mass hierarchy.

Firstly, it was important to check that the event rates of normal and inverted hierarchy of electron appearance are as expected. This was produced by using the initial simulation

produced by GLoBES and taking the event counts of electron appearance rather than the χ^2 . The difference in event rates is visible in Figure 5. Inverted hierarchy gives a different signature, but as they are the same shape this introduces some difficulties discerning between normal and inverted ordering in the event data.

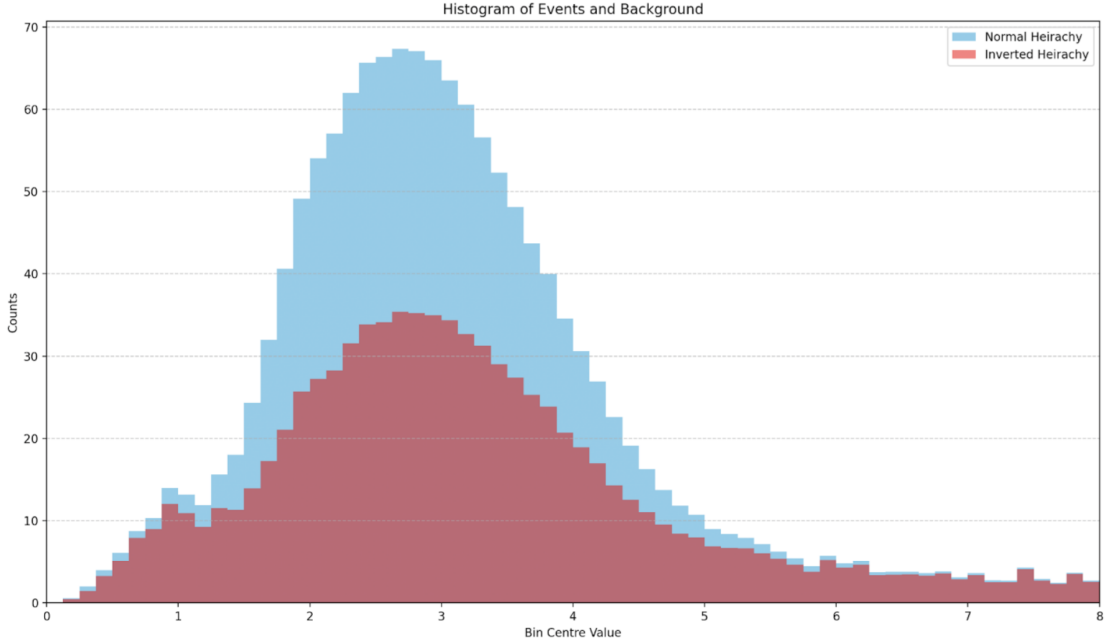


Figure 5: The event rates of normal and inverted hierarchy compared at different bin values (true neutrino energy in GeV), showing a clear distinction. DUNE will be able to contribute to determining whether mass hierarchy is inverted or normal. This graph is considering 3.5 years worth of ν beam and 3.5 years worth of $\bar{\nu}$ beam.

The DUNE technical design report contains predictions about the sensitivity to δ_{CP} (Figure 14). Using the GLoBES simulation, this graph was recreated in Figure 15. Comparing the two graphs shows very similar results, apart from a drop in the simulation in Figure 15 at around $\delta_{CP}/\pi = 0.5$. Sensitivity is higher for low χ^2 values, as is the case at $\delta_{CP}/\pi = 0$. DUNE will have the lowest sensitivity to CP violation when the CP phase is fully in phase with oscillations or in anti-phase. The highest sensitivities are found when the graphs are at a maximum, and when $\frac{\pi}{2}$ out of phase sensitivity reaches the 5σ significance level threshold used in particle physics for confirming new discoveries. The y axis in Figure 15 is the χ^2 value whereas that in Figure 14 is significance level, which is the root mean square of $\Delta\chi^2$.

4.2 Validating the Sterile Neutrino Engine

With all sterile neutrino parameters set to zero, the system acts as it would with 3 neutrinos. This was proven to be the case by comparing the χ^2 distribution over oscillation parameters (in this case δ_{CP}) of these two options, and finding they were identical in Figure 8.

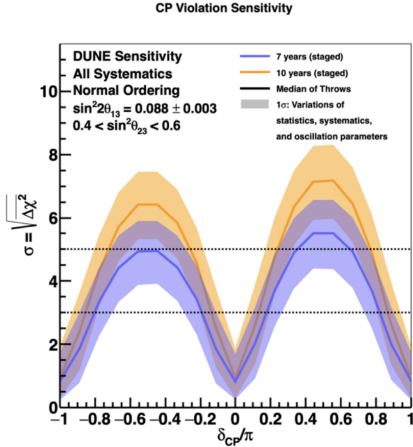


Figure 6: The TDR sensitivity graph of δ_{CP} taken from [19].

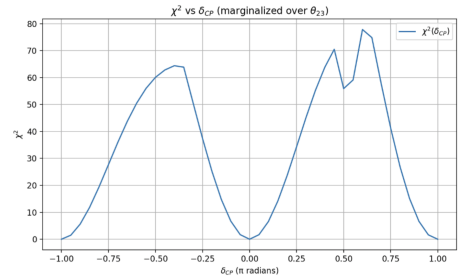


Figure 7: Simulated graph using GLoBES.

The χ^2 values for sterile neutrino parameters were explored - revealing DUNE's potential sensitivity to detecting a sterile neutrino. This was initially done by simulating the far detector - the detector which 'detects' the neutrino oscillations by comparing them to the near detector data (as the initial beam content is not certain). The neutrino parameters of interest were deemed to be Δm_{14}^2 and $\sin^2 \theta_{24}$ - due to having a strong influence on the matrix elements for ν_e appearance and ν_μ disappearance. Figure 9

The specific drop in sensitivity in the lower part of Figure 9 is caused by the atmospheric mass splitting term $\Delta m_{31}^2 \approx 2.5 \times 10^{-3} \text{ eV}^2$ which drives the main effect seen at the far detector. When the sterile mass splitting term (Δm_{41}^2) has a value close to the atmospheric mass splitting term; it can appear as though there has been a change in the three flavour standard neutrino oscillation parameters (most prominently δ_{CP} and θ_{23} [20]). It becomes very difficult to distinguish between the two scenarios in data, and verify a sterile neutrino - hence the loss in sensitivity.

The sensitivity of the far detector overall to sterile neutrino oscillation parameters is affected by large systematic uncertainties. These originate from the beam flux and the interaction cross-section when the beam reaches the far detector. The data taken by the far detector can only be interpreted in relation to that of the near detector - compounding uncertainties.

4.3 Implementing the near detector

The near detector was implemented by adding a new GLoBES file describing the baseline of the near detector and the size (taken to be 20kt despite funding issues that have changed this). There were then 10 globes files spread across the near detector baseline that gave the smeared-source effect present at the near detector. The aim was to verify Figure 10 from the technical design report

The locations of the near detector and beam production facility, as well as the energy spectra of the beam enable DUNE to probe the L/E region 0.01 to 1 eV^2 . As the near detector is so close to the source (574m), there are very high statistics meaning a lot of data is recorded for neutrino interactions. Therefore, there is sensitivity to the

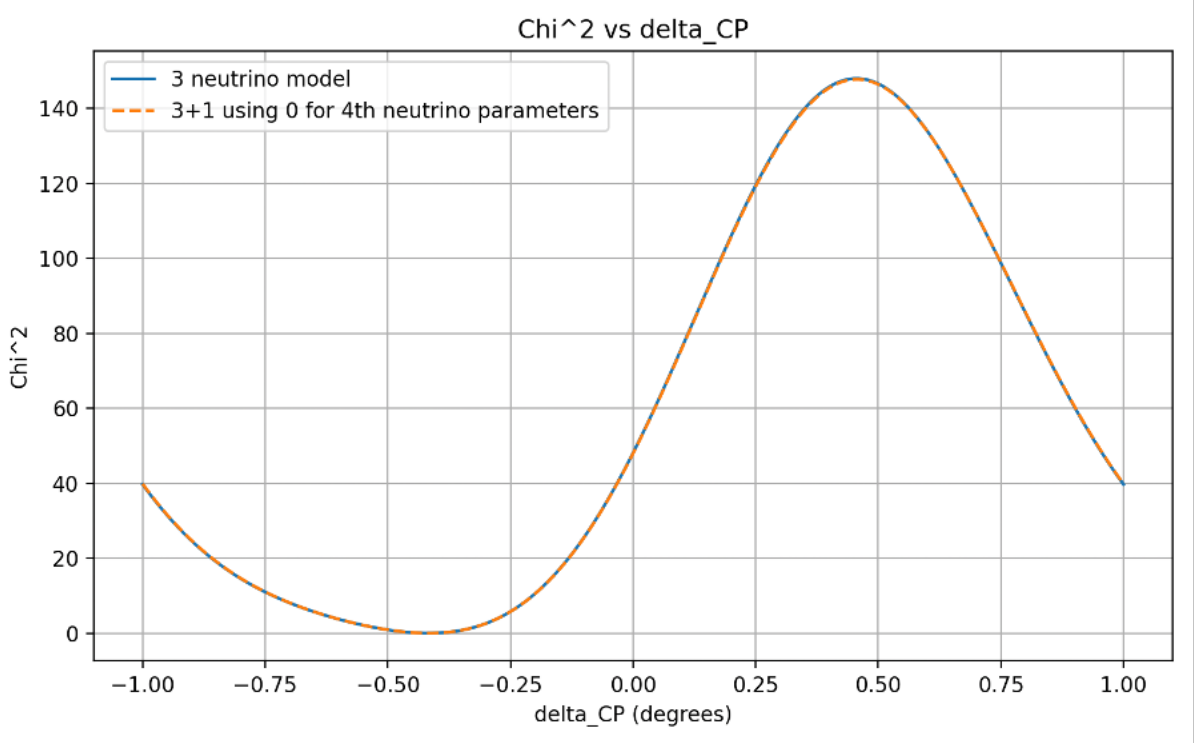


Figure 8: Validation of the null hypothesis working in line with the previous model (standard model) when using the SNU library to simulate a sterile neutrino in GLoBES. The two χ^2 distributions are identical over the parameter space. This graph was marginalised over the parameter θ_{23} .

impact of sterile neutrinos of many of the mixing channels (driven ν_e appearance or ν_τ disappearance, stand-alone ν_μ disappearance or disappearance at the same time as appearance measurements). The graph very easily shifts with different systematics - still owing to the large uncertainties at the far detector.

Figure 11 shows the recreation of the DUNE curve in Figure 10. The characteristic dip in sensitivity due to the atmospheric mass splitting and the increase in sensitivity due to the near detector are both evident. There are also small differences in the shape of the graph - but it is likely due to the systematic errors. There are other factors that could however have had an impact - not limited to the simplifications made in the GLoBES simulations (in this final graph treating the neutrino beam source as a single point)

5 Conclusions

This report has recreated and verified the reproducibility of sensitivity plots for the DUNE experiment. The CP phase δ_{CP} sensitivity in the three neutrino model, as well as sensitivity to neutrino mass ordering, and the existence of a sterile neutrino were explored. It was found that with regard to the sterile neutrino, the DUNE experiment is especially sensitive due to the near detector, and due to the atmospheric mass splitting term, loses sensitivity in another region of the Δm_{14}^2 and $\sin^2 \theta_{24}$ parameter space. The χ^2 statistic

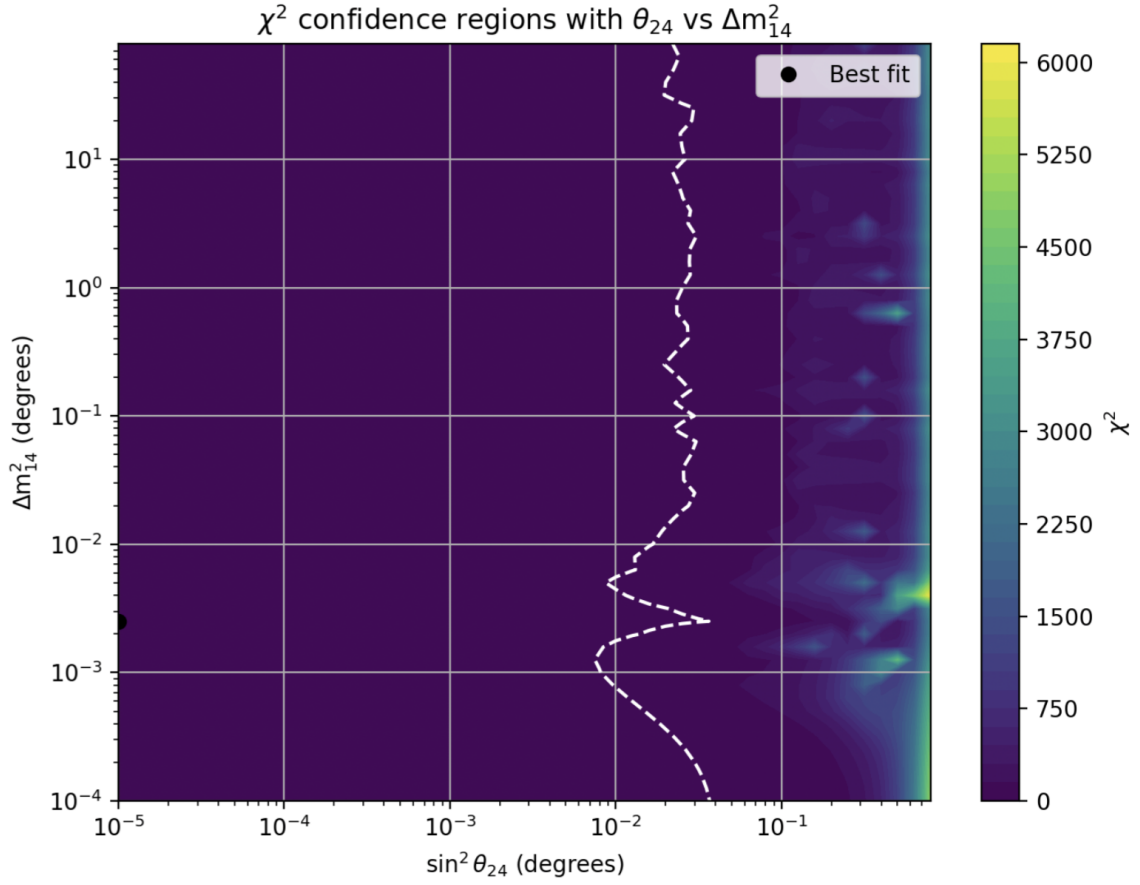


Figure 9: Sensitivity tends to be higher at smaller mass splitting values, however there is a clear drop in this sensitivity around $10^{-2.9}$ where values for $\sin^2 \theta_{24}$ must be an order larger to obtain the same sensitivity.

was used to compare all hypothesis, using GLoBES to calculate these values. DUNE has significantly more sensitivity to these parameters than previous neutrino oscillation detectors, and over the ten year data-taking period, will be able to provide further constraints on values for these parameters, therefore providing novel physical insight into the nature of neutrinos.

References

- [1] B. Abi et. al. Volume i. introduction to dune. *Journal of Instrumentation*, 15(08):T08008, 2020.
- [2] Mona Dentler, Álvaro Hernández-Cabezudo, Joachim Kopp, Pedro Machado, Michele Maltoni, Ivan Martínez-Soler, and Thomas Schwetz. Updated global analysis of neutrino oscillations in the presence of ev-scale sterile neutrinos. *Journal of High Energy Physics*, 2018(8), August 2018.

- [3] Vaia Papadimitriou. Design of the LBNF Beamlne. In *38th International Conference on High Energy Physics*, 2017.
- [4] B. Pontecorvo. Inverse Beta Processes and Nonconservation of Lepton Charge. *Sov. Phys. JETP*, 7:172–173, 1958.
- [5] B. Pontecorvo. Neutrino Experiments and the Problem of Conservation of Leptonic Charge. *Zh. Eksp. Teor. Fiz.*, 53:1717–1725, 1967.
- [6] Y. et. al. Fukuda. Evidence for oscillation of atmospheric neutrinos. *Phys. Rev. Lett.*, 81:1562–1567, Aug 1998.
- [7] L. D. Landau. Possible properties of the neutrino spin. *Zh. Eksp. Teor. Fiz.*, 32:407, 1957.
- [8] Stefano Gariazzo, Martina Gerbino, Thejs Brinckmann, Massimiliano Lattanzi, Olga Mena, Thomas Schwetz, Shouvik Roy Choudhury, Katherine Freese, Steen Hannestad, Christoph A. Ternes, and Mariam Tórtola. Neutrino mass and mass ordering: no conclusive evidence for normal ordering. *Journal of Cosmology and Astroparticle Physics*, 2022(10):010, October 2022.
- [9] C. Marshall. P5 townhall meeting, dune far detectors—phase ii, 2023.
- [10] Basudeb Dasgupta and Joachim Kopp. Sterile neutrinos. *Physics Reports*, 928:1–63, September 2021.
- [11] The DAE δ ALUS Collaboration. The Sterile Neutrino. <https://www.nevis.columbia.edu/daedalus/motiv/sterile.html>, 2025. Accessed: October 2, 2025.
- [12] Igor Krasnov. Dune prospects in the search for sterile neutrinos. *Phys. Rev. D*, 100:075023, 2019.
- [13] Morimitsu Tanimoto and Tsutomu T. Yanagida. Prediction of the CP Phase δ_{CP} in the Neutrino Oscillation and an Axion-less Solution to the Strong CP Problem. *PTEP*, 2025(3):033B01, 2025.
- [14] Patrick Huber, Joachim Kopp, Manfred Lindner, Mark Rolinec, and Walter Winter. Globes: General long baseline experiment simulator. *Computer Physics Communications*, 177(5):439–440, 2007.
- [15] P. Minhas. Dune-globes-simulation-internship-2025 repository, 2025.
- [16] Ivan Esteban, M. C. Gonzalez-Garcia, Michele Maltoni, Ivan Martinez-Soler, and Thomas Schwetz. Nu-fit 6.0: an updated global analysis of three-flavour neutrino oscillations. 7 2024.
- [17] Joachim Kopp. *Sterile neutrinos and non-standard neutrino interactions in GLoBES*. Max-Planck-Institut für Kernphysik, Heidelberg, Germany, 2010. <https://www.mpi-hd.mpg.de/personalhomes/globes/tools/snu-1.0.pdf>.

- [18] K. Abe P. et. al. Sensitivity of the t2k accelerator-based neutrino experiment with an extended run to 20×10^{21} pot, 2016.
- [19] Babak Abi et al. Deep Underground Neutrino Experiment (DUNE), Far Detector Technical Design Report, Volume II: DUNE Physics. 2 2020.
- [20] Dinesh Kumar Singha, Monojit Ghosh, Rudra Majhi, and Rukmani Mohanta. Study of light sterile neutrino at the long-baseline experiment options at km3net. *Phys. Rev. D*, 107:075039, Apr 2023.

A Code

The final code and figures made in this project have been uploaded to GitHub. These can be accessed (complete with comments to explain the logic) at my GitHub here.

B The Sterile Neutrino Implementation in GLoBES

The snu.c and snu.h files were developed by Joachim Kopp [17] in C, and were utilised here to implement a detailed model of the sterile neutrino without doing all the calculations from scratch. The code could work with up to 9 flavours and includes non-standard neutrino interactions (NSI). In all simulations NSI were not considered so most additional parameters (80 of the 92) were set to zero. The remaining non-zero sterile neutrino parameters were those for mass splitting and oscillation phase. When initiating the sterile neutrino engine, three parameters are taken: the number of flavours, the rotation order and the phase order. The neutrino mixing matrix U is made up of rotation matrices: $U = R(\theta_{i_1 j_1}, \delta_k) R(\theta_{i_2 j_2}, \delta_k) \cdots$, where:

$$R(\theta_{ij}, \delta_k) = \begin{pmatrix} 0 & \cdots & 0 & \cdots & 0 & \cdots & 0 \\ \vdots & \ddots & \vdots & & \vdots & & \vdots \\ 0 & \cdots & \cos \theta_{ij} & \cdots & e^{i\delta_k} \sin \theta_{ij} & \cdots & 0 \\ \vdots & & \vdots & \ddots & \vdots & & \vdots \\ 0 & \cdots & -e^{-i\delta_k} \sin \theta_{ij} & \cdots & \cos \theta_{ij} & \cdots & 0 \\ \vdots & & \vdots & & \vdots & \ddots & \vdots \\ 0 & \cdots & 0 & \cdots & 0 & \cdots & 0 \end{pmatrix}$$

The rotation order and phase order are set as follows:

rotation order = $\{\{i_1, j_1\}, \{i_2, j_2\}, \dots\}$

phase order = $\{k_1, k_2, \dots\}$

In this report the following parameters were used to represent a fourth sterile neutrino with this data package. The additional non standard interactions were not utilised - so in this sense this is a simplification.

rotation order = $\{\{3, 4\}, \{2, 4\}, \{1, 4\}, \{2, 3\}, \{1, 3\}, \{1, 2\}\}$

phase order = $\{-1, 2, 1, -1, 0, -1\}$

number of flavours = 4

This was compared to running the standard standard model simulation, and then cross-checked by entering the parameters for the three neutrino model as the SNU parameters and checking that this gives the same result as regular simulation with GLoBES. These parameters are as follows:

rotation order = $\{\{2, 3\}, \{1, 3\}, \{1, 2\}\}$

phase order = $\{-1, 0, -1\}$ and therefore the number of flavours = 3

C The Algorithm

The implementation of the near detector meant accessing multiple GLoBES sheets - one for the near detector and one for the far detector, each with different specifications. The final algorithm includes an additional loop to pass all 10 Near detector sheets through and have a smeared source. One significant issue with this method was that the decay was assumed to occur equally throughout the pipe - before it was altered to have more points further from the detector (as decays happen more frequently at the beginning of the decay pipe). This however was still a rough estimate. The solution would be to fully model the beam pipe facility and to then provide a statistical model to be used in all future simulations. In this algorithm we assume when initialising the GLoBES experiments we are including all of this relevant data.

Algorithm 1 Sterile Neutrino χ^2 Calculation for the DUNE Near Detector

```
1: procedure CALCULATECHISQUARED
2:   Initialise GLoBES experiments (Near and Far Detectors)
3:   Initialise SNU probability engine for 4 neutrino flavours
4:   Register SNU engine with GLoBES
5:   Open output file for writing  $\chi^2$  results
6:            $\triangleright$  Define oscillation parameters for two hypotheses
7:   Define true_values (3-flavour Normal Ordering)
8:   Define test_values (initially set to true_values)
9:   Set prior errors and central values for the fit
10:  Set projection flags (e.g., fix most parameters, keep some free)
11:  Compute event rates based on true_values
12:           $\triangleright$  Scan over the sterile neutrino parameter space
13:  for each value of  $\sin^2(\theta_{24})$  from  $10^{-5}$  to  $10^{-0.1}$  do
14:     $this\_theta24 \leftarrow \arcsin(\sqrt{\sin^2(\theta_{24})})$ 
15:    Set test_values for  $\theta_{24}$ 
16:    for each value of  $\Delta m_{41}^2$  from  $10^{-4}$  to  $10^2$  do
17:      Set test_values for  $\Delta m_{41}^2$ 
18:           $\triangleright$  Calculate the chi-squared for this point in the grid
19:       $\chi_{now}^2 \leftarrow \text{glbChiNP}(\text{test\_values})$      $\triangleright$  Compare sterile hypothesis to null one
20:      Write  $(\sin^2(\theta_{24}), \Delta m_{41}^2, \chi_{now}^2)$  to output file
21:    end for
22:  end for
23:  Close output file
24:  Free all allocated memory (parameters, projections, etc.)
25: end procedure
```

D Further results

Further results from this project not used in this report.

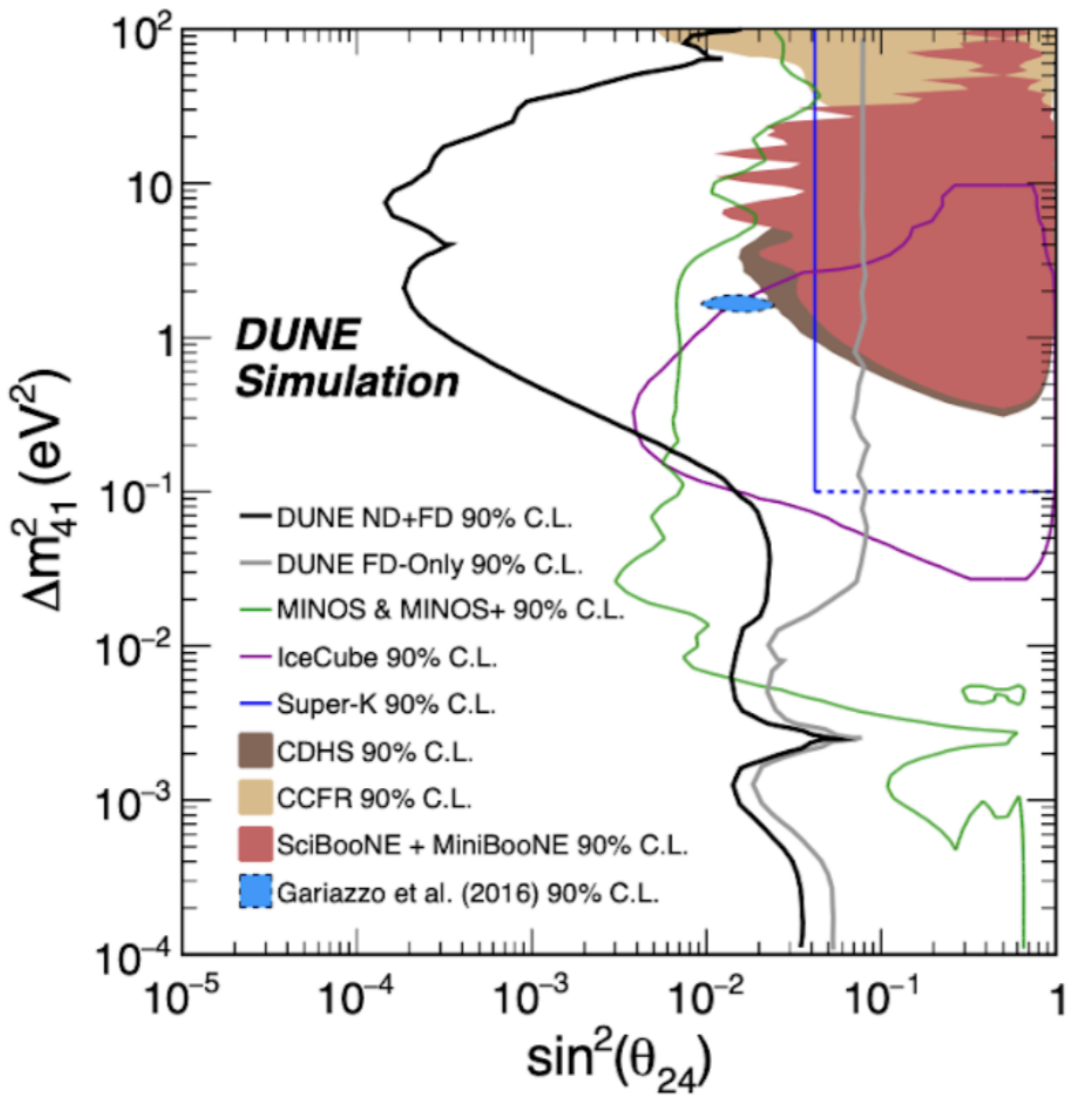


Figure 10: Sensitivity to sterile neutrino parameters at DUNE compared to other experiments as presented in the DUNE TDR in 2020 [19].

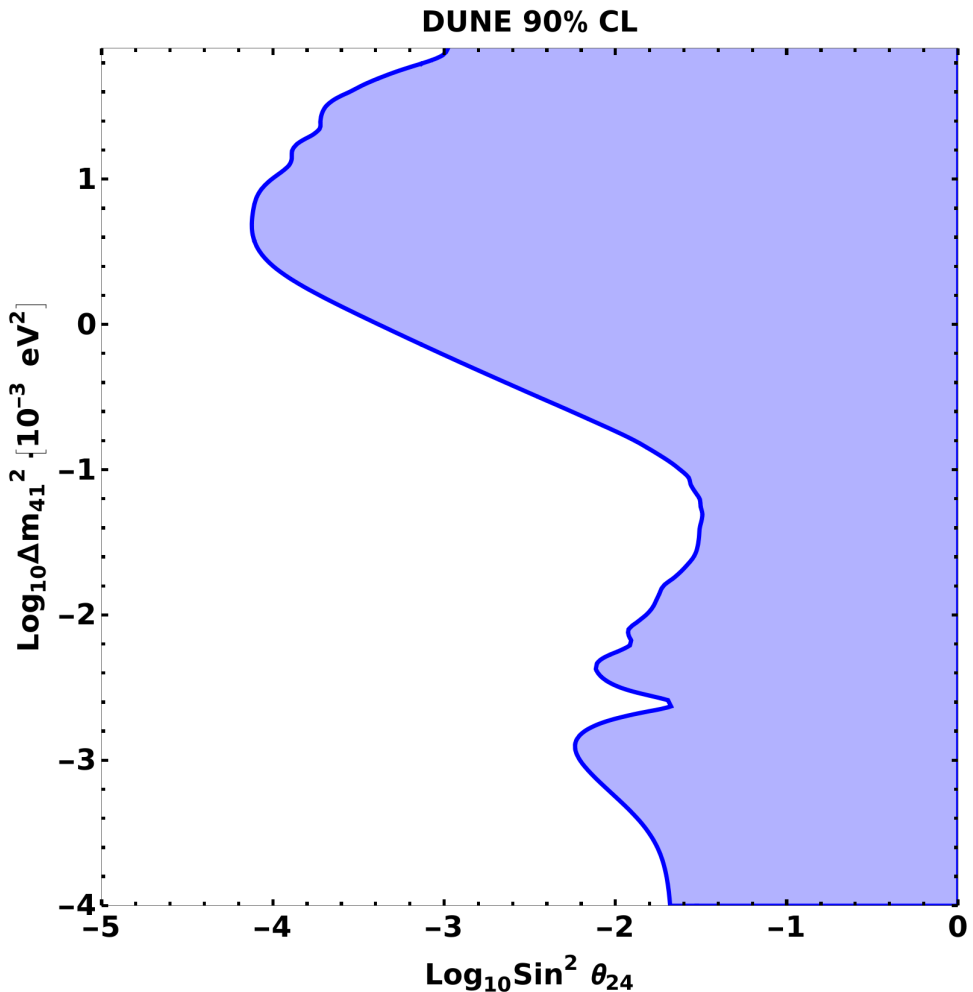


Figure 11: The implementation of the near detector results in greatly increased sensitivity in the range of larger Δm_{14}^2 values, compared to only the far detector. The neutrino source was treated as a single source and not smeared in this particular simulation. See Appendix D for the implementation of the smeared source.

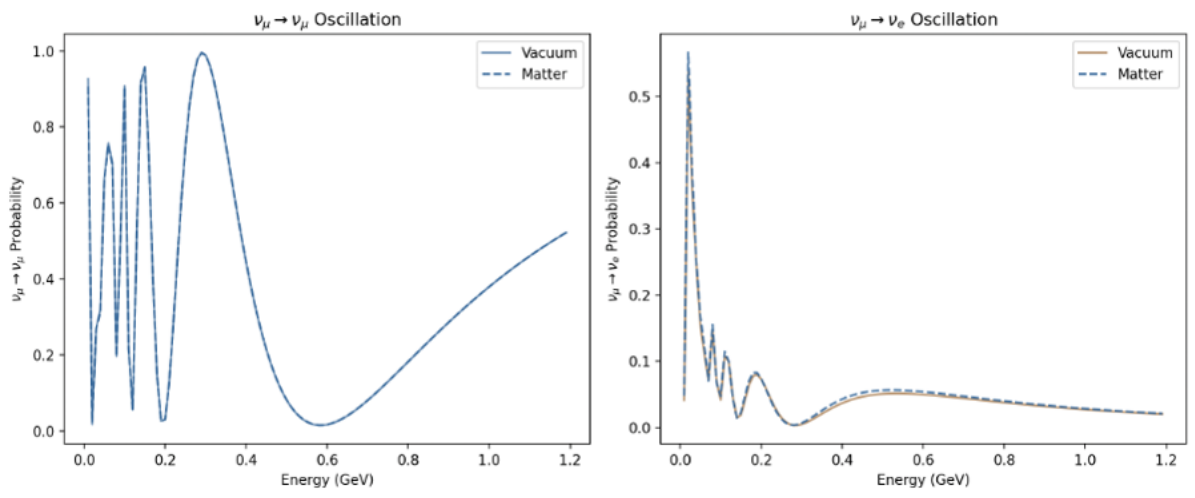


Figure 12: Visualising the matter effect in neutrino oscillation probability at different energies.

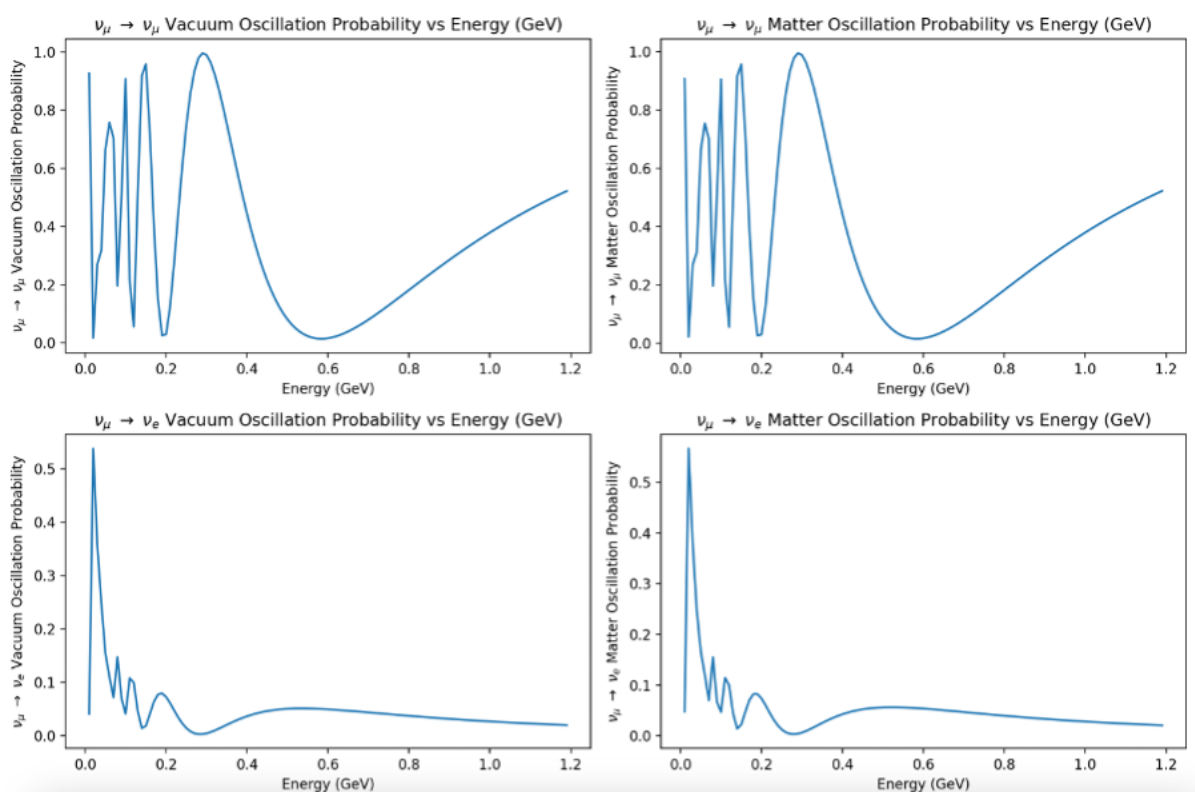


Figure 13: Neutrino oscillation probabilities in a vacuum for appearance and disappearance.

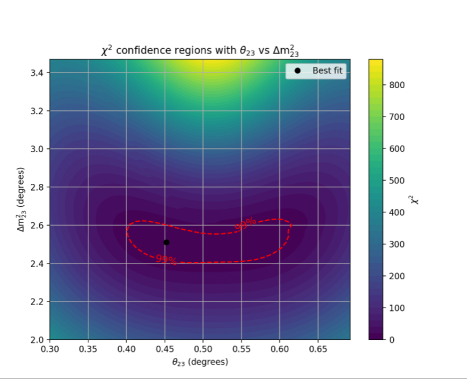


Figure 14: The sensitivity to normal and inverted mass ordering at the T2K detectors (Tokai to Kamioka).

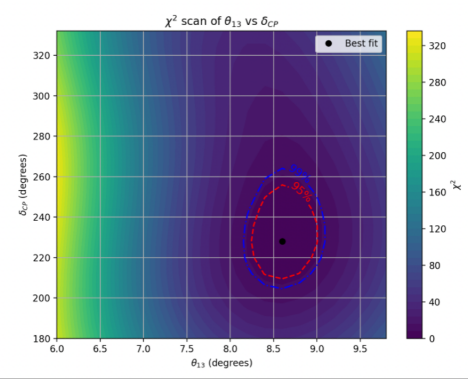


Figure 15: Simulated χ^2 sensitivity matrix for a simulated 50kt liquid scintillator detector being ran for 6 years.

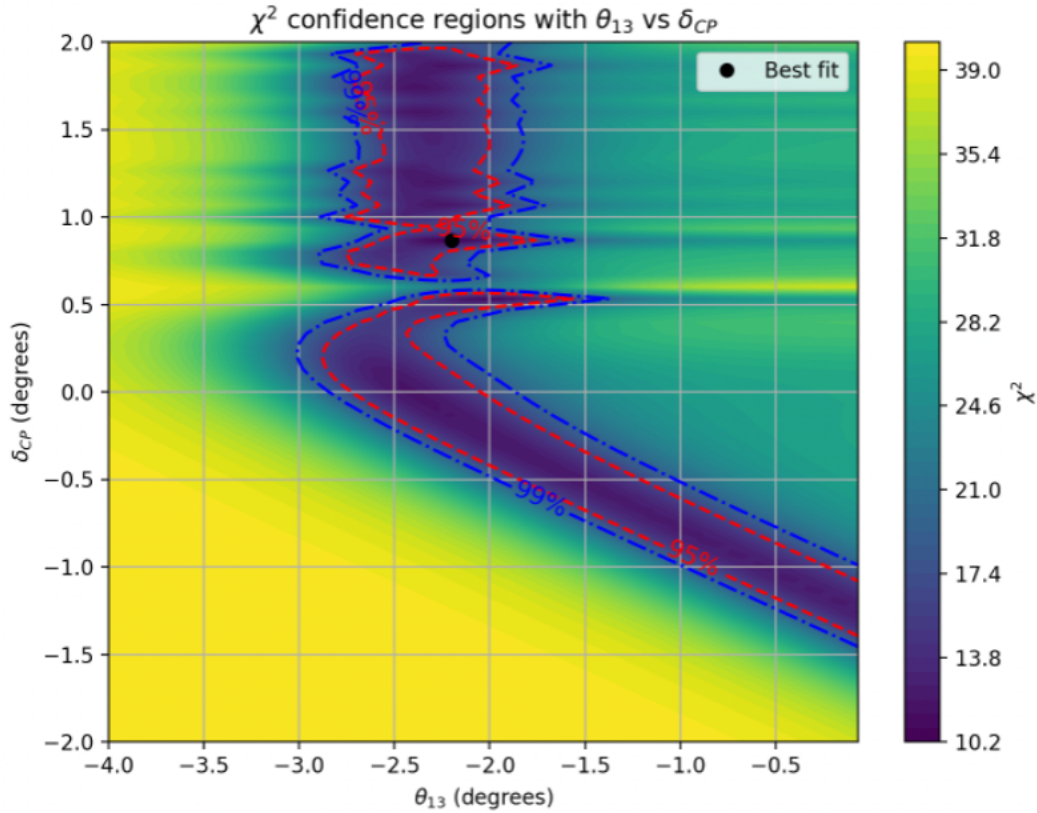
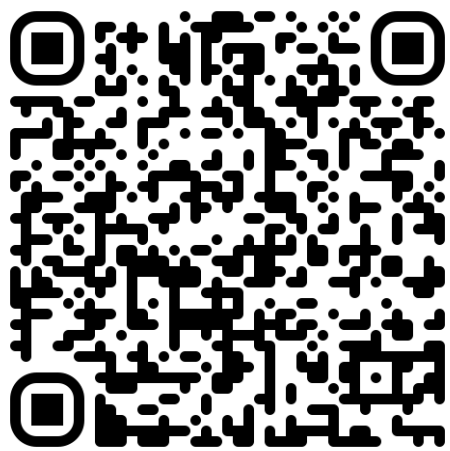


Figure 16: The effect on sensitivity to neutrino oscillation parameters at LSND (Liquid Scintillator Neutrino Detector) by implementing a 3+1 neutrino model.



A QR code linking to the GitHub repository for this project.